latitude magnetometer networks or chains and are sensitive to polar region current systems including the auroral electrojet.

With the increasing importance of satellites and spacecraft for commerical and military purposes has come an increasing interest in *forecasting* space weather. The interested reader is referred to the recent review, "Geomagnetic Activity Forecasting: The State of the Art," by J. Joselyn (1995). Joselyn writes:

> The level of disturbance of the space environment is of more than academic interest. Such private and public endeavors as communication and navigation systems, electric power networks, geophysical exploration, spacecraft control, and science research campaigns are affected by geomagnetic fluctuations.

In order to make space weather forecasts, solar conditions, such as flares, sunspot groups, and especially CMEs, are closely monitored as is the solar wind. The Space Environment Laboratory (SEL) of the National Oceanic and Atmospheric Administration (NOAA) in Boulder, Colorado, issues daily reports and forecasts of geomagnetic activity.

8.7 Magnetospheres of the outer planets

8.7.1 A brief overview

Our knowledge of the outer planets has largely been derived from data generated by NASA's *Pioneer* and *Voyager 1* and *2* missions. Jupiter was visited by the *Pioneer 10* and *11* spacecraft and also the *Voyager 1* and *2* spacecraft. *Pioneer 11* and *Voyagers 1* and *2* flew by Saturn, and both Uranus and Neptune were encountered by *Voyager 2*. More recently, the *Ulysses* spacecraft, launched in October 1990, encountered Jupiter in February 1992 on its way out of the ecliptic plane, and in December 1995 NASA's *Galileo* spacecraft went into orbit around Jupiter and the probe plunged into the Jovian atmosphere. All these spacecraft carry thermal and energetic particle detectors, magnetometers, plasma wave detectors, and radio receivers. Reviews of our understanding of outer planet magnetospheres are listed at the end of this chapter (Bagenal, 1985, 1992; and articles in the book *Physics of the Jovian Magnetosphere* edited by Dessler).

The outer planets (Jupiter, Saturn, Uranus, and Neptune) all possess large intrinsic magnetic fields that play central roles in the interactions of these planets with the solar wind. (See Table 7.1 for planetary characteristics including magnetic dipole moments and rotation periods.) The planetary fields are not purely dipole fields, but include higher-order moments, and the magnetic dipoles are not in general aligned with the rotation axes. Figure 8.50, which was adapted from a figure in the article by Bagenal (1992), summarizes schematically the differences between the outer planets in this regard. The *obliquity* is the angle between the rotation axis and the vector normal to the ecliptic plane. For Earth, the obliquity is 23.5 degrees. The tilt angle of the magnetic dipole with respect to the rotation axis is also indicated

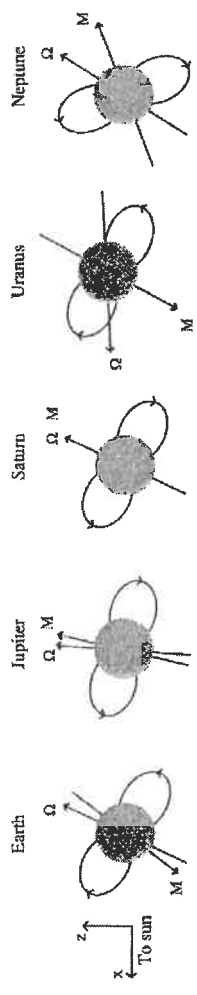

Figure 8.50. Schematic of magnetic field and rotation of the outer planets. **M** is the dipole moment; **Ω** is the angular frequency. The dipole tilt angle is the angle between **M** and **Ω**. Adapted from Bagenal (1992).

in Figure 8.50. Clearly, the Jovian and Saturnian magnetic fields are qualitatively similar to Earth's, whereas the magnetic fields of Uranus and Neptune are rather irregular. The magnetic field patterns of Uranus and Neptune change drastically over the course of a rotation period, unlike Earth, Jupiter, and Saturn. Uranus and Neptune are said (cf. Bagenal, 1992) to have *asymmetric magnetospheres*. The topologies of these two magnetospheres are quite complex.

The magnetospheres of the outer planets are all quite large. Putting aside details of the structure of each magnetosphere, we estimated the distance to each outer planet magnetopause using Chapman–Ferraro theory in Chapter 7. The radial distance to the Jovian magnetopause is observed to be $r_{mp} \approx 50$–$100\ R_J$. The Jovian magnetosphere is indeed huge considering that the Jovian radius R_J is 12 R_E. Simple Chapman–Ferraro theory, which balances internal magnetic pressure against solar wind dynamic pressure, gave (in Chapter 7) a Jovian magnetopause distance of only about 30 R_J. Internal plasma pressure associated with the plasmasheet (with $\beta \approx 5$) was invoked (Equation (7.14)) to supply extra internal pressure and push the magnetopause further out. In contrast, the distance to the terrestrial subsolar magnetopause ($r_{mp} \approx 10\ R_E$) was quite well described by the simple theory. It happens that the magnetopause distances of Saturn, Uranus, and Neptune are all reasonably accurately determined by the simple theory (you were asked to do this back in Problem 7.3 using Equation (7.10)). The observed magnetopause distances are approximately: 20 R_S for Saturn, 18 R_U for Uranus, and 25 R_N for Neptune. The planetary radii of Saturn, Uranus, and Neptune are denoted R_S, R_U, and R_N, respectively.

The outer planets all rotate rapidly, and the magnetospheres are largely dominated by rotational plasma flow. This can be seen by comparing the *corotational electric field* $\mathbf{E}_{cor}$ with the *convection electric field* $\mathbf{E}_m$, as was done for the terrestrial magnetosphere in Section 8.4.3. The magnitude of $\mathbf{E}_{cor}$ for the terrestrial magnetosphere was given by Equation (8.85). Generalizing this formula to planet "x" (with angular frequency Ω_x, surface field B_x, and radius R_x) we obtain for the equatorial plane ($\theta = 90°$)

$$E_{cor} = \Omega_x B_x R_x^3 / r^2, \tag{8.117}$$

where r is the radial distance from the center of the planet. As discussed in Section 8.4.3, E_{cor} decreases as r^{-2} whereas E_m is roughly a constant; this means that at a small enough radial distance corotation must dominate over magnetospheric plasma convection. The convection electric field can be estimated using Equation (8.3) and is $E_m = \zeta u_{sw} B_0$, where B_0 is the IMF strength at the heliocentric distance of planet x, u_{sw} is the solar wind speed, and ζ is the efficiency of the dayside magnetic reconnection process for the magnetosphere.

Recall that the region of the terrestrial magnetosphere where the plasma corotates with the Earth is called the plasmasphere. The plasma density in this region remains high relative to the portion of the magnetosphere outside where plasma is lost by

Table 8.2. *Theoretical plasmapause L-shell values*

	Jupiter	Saturn	Uranus	Neptune
L_{pp}	240	70	50	50

being convected to the dayside magnetopause. The radial distance to the boundary of the plasmapause was given by Equation (8.88), which was found by equating E_{cor} and E_m and then solving for the plasmapause L-shell value, L_{pp}. Generalizing this equation using Equation (8.117) and recognizing that $\Psi_m \approx 3 r_{mp} E_m$, we obtain the following relation for L_{pp}:

$$L_{pp} \cong \sqrt{\frac{\Omega_x B_x R_x}{E_m}} = \sqrt{\frac{\Omega_x B_x R_x}{\zeta u_{sw} B_0}}. \tag{8.118}$$

This formula can be used to estimate the sizes of the corotating region (i.e., the plasmasphere) for the outer planets by using the parameters listed in Table 7.1. (See Problem 8.25.) The surface fields of Jupiter, Saturn, Uranus, and Neptune are approximately 40, 2, 2.5, and 1.4×10^{-5} T, respectively. Note that the IMF field strength B_0 decreases with heliospheric distance as discussed in Chapter 6. A question arises as to what values of the reconnection efficiency ζ are appropriate for the outer planets, but simply using a reasonable terrestrial value ($\zeta = 0.2$) for moderately active times we find the values of L_{pp} for the outer planets as shown in Table 8.2.

For Earth, Equation (8.118) gives $L_{pp} = 5.5$. Now we compare these plasmapause L-values with the size of the magnetosphere (i.e., with r_{mp} or r_{mp}/R_x). For Earth, $r_{mp} = 10\ R_E$, but the distance to the plasmapause is about half of this or 5.5 R_E. A large volume of the magnetosphere lies outside the plasmapause, even on the dayside, and for most of the magnetosphere the plasma dynamics is controlled by solar wind–driven convection. However, from the above comparisons for the outer planets we see that the radial size of the corotating region is about 2–4 times greater than the radial distance to the magnetopause, which is clearly impossible. What this means is that corotation dominates the plasma dynamics of these planets all the way out to the magnetopause! There is "no space" left for solar wind–driven plasma convection to take place, at least in the equatorial plane. This is an oversimplification, and solar wind–driven convection must still play some role at very high magnetic latitudes, deep in the magnetotail, and/or in a narrow boundary layer just inside the magnetopause. Clearly, the magnetospheric dynamics of the outer planets is quite different from the dynamics at the Earth or Mercury.

Bagenal (1985, 1992) has summarized the properties of the magnetospheric plasma of the outer planets. The thermal plasma in the magnetospheres of the outer

planets, or at Earth for that matter, is approximately Maxwellian with temperatures in the several eV to several keV range, depending on location. However, the typical densities in these magnetospheres are quite different. The maximum magnetospheric plasma density is ≈1,000–5,000 cm^{-3} at both Jupiter and the Earth (i.e., in the plasmasphere), whereas for Saturn the maximum density is $n_e \approx 100\,cm^{-3}$. The maximum thermal density in the magnetospheres of both Uranus and Neptune is quite small – only about 3 cm^{-3}.

Where does this plasma come from? Recall that the source of plasma for the terrestrial magnetosphere is both the solar wind and the ionosphere. For the outer planets these two sources still contribute plasma, but an even more important source exists: the satellites of these planets, most of whose orbits lie within these very large magnetospheres. For example, for Jupiter the most important source of both thermal, and ultimately the energetic plasma, is the innermost Galilean moon Io, although the icy satellites Ganymede, Europa, and Callisto are also thought to act as plasma sources. The *Voyager* spacecraft measured large abundances of sulfur and oxygen ions both in the thermal plasma and in the energetic radiation belt ion population; this is a clear indicator of an Io plasma source since we know that Io has a thin SO_2 atmosphere that appears to be replenished by volcanic activity. The important plasma sources at Saturn include the satellite Titan, which has a dense nitrogen atmosphere and contributes nitrogen ions to the outer magnetosphere; the icy satellites; and the rings, which contribute both oxygen ions and protons to the inner magnetosphere. Similarly, Neptune's satellite Triton acts as a source of nitrogen ions for that magnetosphere, although the thinner, colder atmosphere of Triton, in comparison with Titan, somewhat limits this source. The satellite source of plasma for Uranus is rather weak, consisting of rather small satellites and thin ring arcs.

The outer planets all have radiation belts containing energetic ions and electrons. The phase space densities of MeV energy range ions (heavy ions as well as protons) in the radiation belts of Earth and Saturn are comparable, but the radiation intensities at Jupiter are more than a factor of 10 greater than they are at Earth. The radiation belts of Uranus and Neptune are rather puny with intensities 10 times less than at Earth.

8.7.2 The Jovian magnetosphere and the Io plasma torus

The following ion species have been observed by spacecraft in the thermal plasma of the Jovian magnetosphere (e.g., Geiss et al., 1992): H^+, He^{++}, and O^{6+} of solar wind origin; H^+, H_2^+, and H_3^+, originating from the Jovian ionosphere; and S^{2+}, S^{3+}, S^{4+}, S^{5+}, O^+, O^{2+}, and O^{3+}, originating from Jupiter's satellite Io. The S and O ion species are especially abundant, particularly in the inner ($L < 10$) and middle ($L < 40$) regions of the magnetosphere. The densest part of the inner magnetosphere is called the *Io plasma torus*. The thermal electron gas in this torus has a temperature of about 200 eV. The composition of the energetic plasma population

(i.e., the plasma whose particles have energies in excess of about 10 keV/amu) is also dominated by S and O species (cf. Lanzerotti et al., 1992). Energetic electrons with energies in excess of 100 keV are also present in the Jovian magnetosphere, and radiation belt particles with energies in the 1–100 MeV range have also been observed.

Io is a very important source of plasma for the Jovian magnetosphere. The orbital radius of Io is 5.9 R_J. Sulfur dioxide (SO_2) is released into the tenuous atmosphere of that body by volcanoes; some of these volcanoes were actually observed erupting by the *Voyager* television camera. Exospheric SO_2 molecules are able to escape the gravitational field of Io and move into the magnetosphere of Jupiter where they are ionized and dissociated by magnetospheric electrons, resulting in the creation of sulfur and oxygen ions. Charge transfer and electron removal collisions largely determine the distribution of ion charge states for S and O in the Io plasma torus. In some respects this is analogous to the solar corona, where collisions act to set up a distribution of charge states for the various ion species. The ultraviolet spectrometers on the *Voyager* spacecraft observed ultraviolet emissions from the Io plasma torus associated with the various S and O charge states.

Neutral particles in the Jovian magnetosphere do not "see" Jupiter's magnetic field or the corotation electric field. However, once the neutrals are ionized, the ions that are produced experience the Lorentz force and are "picked up" by the corotating Jovian magnetic field. The pickup process is essentially the same as we discussed in Chapter 7 with respect to cometary ions picked up by the solar wind. The newly born ions $\mathbf{E} \times \mathbf{B}$ drift at a speed slightly less then the corotation speed. In the case of comets, this speed was the solar wind speed rather than the corotation speed. The newly born ions are "hot" because the amplitude of their gyration is approximately equal to the corotation speed (73 km/s) minus the orbital speed of Io (16 km/s). The orbital speed is the average speed the neutrals have before they are ionized. New oxygen and sulfur ions acquire energies of 260 eV and 540 eV, respectively. The Io plasma torus is not collisionless, however, and this pickup gyration energy is eventually shared with the rest of the plasma via Coulomb collisions. Thus, the plasma as a whole is heated via the pickup process. The total energy input into the Io plasma torus from this process is just the total ion addition rate multiplied by the average pickup energy.

The total Io source of heavy ions is $S_{Io} \approx 10^{28}$–10^{29} ions/s, and the resulting heating rate is $\approx 400\,eV \times S_{Io} \approx (0.5\text{–}5) \times 10^{31}$ eV/s $\approx (0.8\text{–}8) \times 10^{12}$ W. The total energy loss associated with the observed radiation for S and O species from the torus is roughly 10^{13} W, which is comparable to the estimated energy input rate. The energetics of the Io plasma torus are not fully understood, but as with all such problems it is necessary that energy inputs, energy losses (such as radiation), and energy transport all be balanced.

Figure 8.51 shows *Voyager 1* electron density data (same as total ion density) and ion temperature (T_i) data for the Io plasma torus. The torus can be divided into

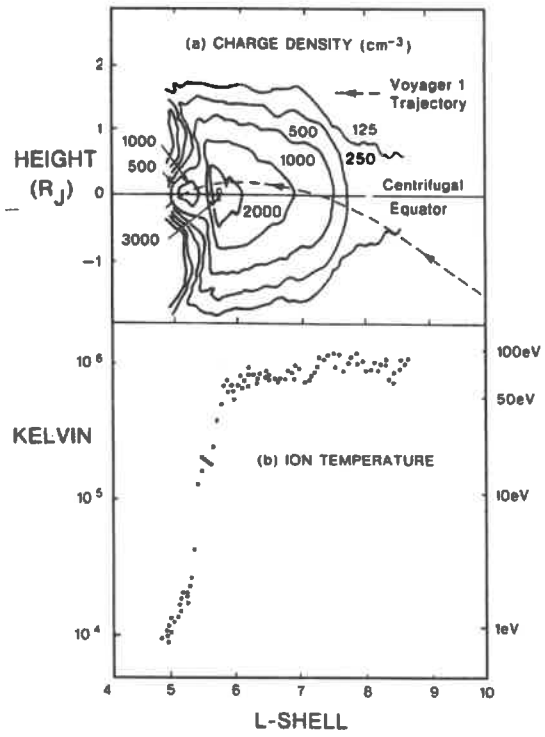

Figure 8.51. (Top panel) Contours of electron density versus L-shell and height from the equatorial plane of the magnetosphere, as determined from plasma measurements made by *Voyager 1* in the Io plasma torus. (Lower panel) Ion temperature in the equator. (From Bagenal, 1985.) Copyright 1985 Kluwer Academic Publishers. With kind permission from Kluwer Academic Publishers.

two parts: (1) an *inner cold torus* where the ion temperature $T_i \approx 1$ eV for $L < 5.7$ and (2) an *outer warm torus* for $L > 5.7$ where $T_i \approx 100$ eV. The ion temperature (or thermal energy) in the warm torus is somewhat less than the pickup energy, which is not surprising given that energy is lost by processes such as radiation. The electron density profile exhibits a maximum on the "rotational" equator of the magnetosphere, and the density decreases with height above or below this equatorial plane. The vertical scale height in the cold torus is quite small, but in the outer torus the scale height is larger with $H \approx 1 R_J$. The maximum electron density in the torus is about 2,000 cm^{-3} and occurs at $L \approx 6$. The density decreases to about 250 cm^{-3} by an L-shell of $L \approx 8$.

8.7.3 Dynamics of the Jovian magnetosphere

In this section, we briefly consider the dynamics of the Jovian magnetosphere using the same methods that were used earlier to explain the terrestrial magnetospheric dynamics. We will consider the force balance or dynamics of the inner and middle Jovian magnetosphere and will not discuss the outer magnetosphere ($L > 40$) or the magnetotail. The plasma essentially corotates, but we need to determine how the corotation is maintained and what electrical currents flow in the magnetosphere in response to the momentum balance. Again, the slab example presented in Section 8.3 can help us to understand this problem.

Before proceeding, we should ask ourselves if the currents can be found using simple MHD theory as discussed in Section 8.3. In the Earth's plasmasheet this theory with isotropic pressure worked reasonably well, although the pressure is not entirely isotropic (Figure 8.40); however, to understand the ring current in the inner magnetosphere we needed to include gradient and curvature drifts, which required (as discussed in Chapter 3) a separate consideration of perpendicular and parallel pressures for the energetic ring current plasma. Furthermore, in the inner magnetosphere of the Earth most of the total particle density (as opposed to the pressure) is associated with the colder (≈1 eV) thermal plasma within the plasmasphere for which convection (i.e., $\mathbf{E} \times \mathbf{B}$ drift motion) is more important than gradient and curvature drifts. We now derive a critical energy (or speed) for ions at which their $\mathbf{E} \times \mathbf{B}$ drift speed equals their gradient and curvature drift speed. Ions with speeds less than this critical speed mainly undergo $\mathbf{E} \times \mathbf{B}$ drift, and the dynamics can be described with simple single-fluid MHD theory with isotropic pressure, whereas ions with speeds greater than this critical speed also undergo gradient and curvature drift.

We use the corotation speed for the $\mathbf{E} \times \mathbf{B}$ drift speed ($v_E = v_{corot}$), in which case the critical speed can be determined from the condition $v_B = v_{corot}$. Recall from Chapter 3 that the gradient and curvature drift speed, v_B, depends on the total particle energy (Equation (3.34) or (3.76)). You will find from doing Problem 8.24 that the critical particle speed is roughly given by $v_{crit}^2 \approx \Omega_{gyro}\Omega_{rotation}R_x^2L^2$, where we have distinguished in our notation between the gyrofrequency Ω_{gyro} and planetary rotational frequency $\Omega_{rotation}$. R_x is the relevant planetary radius for planet "x" and L is the L-shell. For both protons and oxygen ions at $L \approx 6$ in the terrestrial magnetosphere the "critical" energy is roughly $E_{crit} \approx 10$ keV. Above this "critical" energy, the proton motion, and any associated electrical currents, is dominated by single particle gradient and curvature drifts; below this energy, the proton motion is determined mainly by $\mathbf{E} \times \mathbf{B}$ convection. The L-shell value $L \approx 6$ corresponds to the outer part of the terrestrial ring current region or to the inner edge of the plasmasheet. At Earth the total plasma pressure near $L \approx 6$ is dominated by the ring current population, and the electrical current (and "dynamics") for this component is determined by gradient and curvature drift motion since the average ring current energy $E \gg E_{crit}$. However, at larger L-values where $E < E_{crit}$, the pressure in the

plasmasheet of Earth is carried by ions with energies of a few keV, and the simpler MHD theory with isotropic pressure works reasonably well, albeit not perfectly.

For Jupiter, do we need to worry about the electrical currents associated with single particle gradient and curvature drifts, or will the simpler MHD theory work reasonably well? Consider an L-shell of 10, which is roughly the boundary between the outer Io plasma torus and the middle magnetosphere. The critical energy for an oxygen ion at $L \approx 10$ is about 15 MeV! "Cold" thermal plasma particles near $L \approx 10$ have energies of about $T_i \approx 100$ eV, and even the more energetic particles that carry most of the pressure near $L \approx 10$ (the equivalent of terrestrial ring current plasma) have typical energies of only 100 keV/amu; thus, $E \ll E_{\text{crit}}$. In other words, convection due to E_{corot} is more important for this Jovian "ring current" energetic plasma than are gradient and curvature drifts, unlike the Earth's ring current plasma. Only radiation belt particles in the Jovian magnetosphere, with energies in excess of about 15 MeV, are controlled by gradient and curvature drifts for $L \approx 10$, but these particles do *not* contribute a significant fraction of the total pressure.

Now we continue with our discussion of the Jovian magnetospheric dynamics, restricting ourselves to simple MHD theory. The momentum equation (8.28) is a good starting point. This equation includes a mass-loading term that is proportional to the ion production rate P_i multiplied by $(\mathbf{u} - \mathbf{u}_n)$. For the case of the Io plasma torus, $\mathbf{u}_n$ should be identified as the orbital speed of Io (the speed at which the neutrals are injected into the magnetosphere), and $\mathbf{u}$ is the plasma flow velocity; at the orbit of Io we have $|\mathbf{u} - \mathbf{u}_n| = 57$ km/s. Recall from the section on comets in Chapter 7 that mass-loading slows down a plasma; hence, the addition of sulfur and oxygen ions to the Io plasma torus should result in plasma flow that is at least a little slower than the corotation speed. Actually, the plasma flow is very close to corotation, at least for $L < 40$. That is $\mathbf{u} = \boldsymbol{\Omega} \times \mathbf{r}$ is a good description of the plasma motion, where $\boldsymbol{\Omega}$ is the same as $\boldsymbol{\Omega}_{\text{rotation}}$, and the momentum balance in the corotation frame of reference is an almost static balance. The plasma density and particle distribution functions are largely controlled, not by bulk radial plasma flow, but by slow radial diffusion. The right-hand side of Equation (8.28) for steady-state conditions and in a *corotating coordinate system* becomes

$$\rho\boldsymbol{\Omega} \times (\boldsymbol{\Omega} \times \mathbf{r}) \cong -\nabla p + \mathbf{J} \times \mathbf{B} - P_i m_i (\mathbf{u} - \mathbf{u}_n). \tag{8.119}$$

The left-hand side of Equation (8.119) is just the centripetal force per unit volume of the plasma. This MHD force balance equation can be separated into its radial, azimuthal, and vertical components. Vertical is with respect to the rotational equatorial plane. We now consider each of these components individually.

8.7.3.1 *Azimuthal force balance*

If we assume that the Jovian magnetosphere (and plasma pressure) is symmetric about the rotation axis, then $\partial p/\partial\phi = 0$ and since $-\boldsymbol{\Omega} \times (\boldsymbol{\Omega} \times \mathbf{r})$ is directed radially outward and does not contribute to the azimuthal force balance, the azimuthal

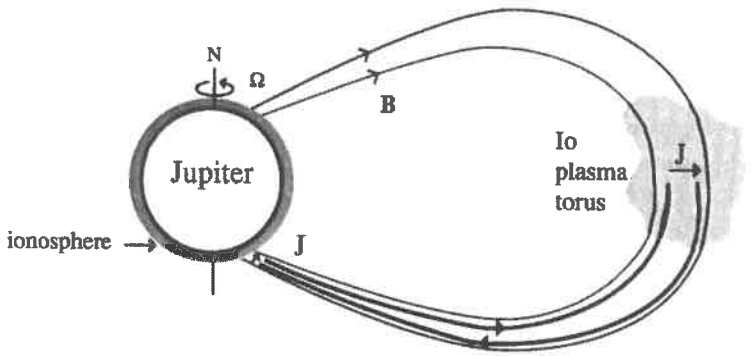

Figure 8.52. Current system associated with azimuthal MHD force balance in the Io plasma torus. Mass-loading from ion production requires a radial electrical current, which then flows as Birkeland currents along the magnetic field and closes in the Jovian ionosphere as Pederson currents.

component of Equation (8.119) simply becomes

$$J_r B \cong P_i m_i (u - u_n) \cong P_i m_i \Omega r, \tag{8.120}$$

where J_r is the radial current density and where we have also made the approximation that $u \gg u_n$. Here Ω is Ω_{rot}. Clearly, the radial current density depends on both the rotational frequency of Jupiter and on the ion production rate. Equation (8.120) just states that a radially directed electrical current is needed so that the $\mathbf{J} \times \mathbf{B}$ force can balance the momentum addition due to ion production. Figure 8.52 illustrates the current system associated with mass-loading in the Io plasma torus. Charge conservation (i.e., Kirchoff's current law) requires that the electrical current come from somewhere and go somewhere. Parallel electrical currents, or Birkeland currents ($J_\parallel$), are thus required, just as was discussed earlier in this chapter for the simple example with two slabs connected by a magnetic field. The electrical "circuit" closes in the ionosphere as Pederson currents. The resulting $\mathbf{J} \times \mathbf{B}$ force in the Jovian ionosphere acts to slow the plasma flow down relative to the corotating neutral atmosphere. This actually reduces the corotation electric field a little, and thus the plasma flow in the Io plasma torus is also a little slower than (that is, it lags) the corotation speed. In the ionosphere, the $\mathbf{J} \times \mathbf{B}$ force is balanced by ion–neutral drag. Some quantitative details on mass-loading effects in the Io torus are provided in the next two examples.

Example 8.5 (Total current flowing in "mass-loading electrical circuit" pictured in Figure 8.52) The total radial electrical current can be found from Equation (8.120) by integrating J_r over the cross-sectional area of the plasma torus,

which can roughly be described as a circle around Jupiter with circumference $2\pi L R_J$, where $L \approx 6$, and with a vertical extent $\Delta z \approx 2R_J$. Thus,

$$I \approx 2\pi L R_J \Delta z J_r \approx 4\pi L^2 R_J^3 \Omega P_i m_i / B. \tag{8.121}$$

Approximately, we can represent the magnetic field strength with a dipole value, $B \approx B_J/L^3$. The rotational frequency is denoted $\Omega = \Omega_J$. The total ion production rate throughout the entire Io plasma torus is just the volume integral of the local production rate P_i, or $S_{Io} \approx 2\pi L R_J^2 \Delta z \Delta L P_i$, where ΔL is the radial extent of the region with significant mass addition. Equation (8.121) now becomes

$$I \approx \frac{L^4}{\Delta L} \frac{m_i S_{Io} \Omega}{B_J}. \tag{8.122}$$

Substituting reasonable values for the parameters ($L = 6$, $\Delta L = 2$, $S_{Io} = 3 \times 10^{28}\ s^{-1}$, $\langle m_i \rangle \approx 25$ amu, $B \approx 5 \times 10^{-4}$ T), Equation (8.122) predicts that the total current in this system is $I \approx 1$ MA.

Example 8.6 (Departure of the plasma convection speed from the corotation speed in the Io plasma torus) In the ionospheric part of the "electric circuit" shown in Figure 8.52 the current density can be denoted $J_{\perp iono}$ and flows in the part of ionosphere connected via magnetic field lines to the Io plasma torus (i.e., at about 65° latitude). The force balance equation in the ionosphere can be written as $J_{\perp iono} B_J = \rho_{iono} \nu_{iono} (u - u_n)$, where the neutrals can be assumed to be, in the absence of any upper atmospheric winds, corotating with Jupiter: $u_n \approx \Omega R_J$. The ion–neutral collision frequency is denoted ν_{iono}. The departure from corotation is $\Delta u = u - u_n \approx J_{\perp iono} B_J / (\rho_{iono} \nu_{iono})$. The current density can be found by using the total current estimated in the previous example and by applying an appropriate ionospheric geometry. If there were no mass-loading in the magnetosphere, then there would be no current and $J_{\perp iono} = 0$. In this case, $u = u_n$; no departure from corotation would be present. On the other hand, the presence of a current results in a finite value of the corotation lag Δu.

A better way (but equivalent) of determining Δu is to calculate the height-integrated Pederson current density $K_\perp \approx J_{\perp iono} H_{iono}$ using the height-integrated conductivity $\Sigma_{\perp iono}$ for the Jovian ionosphere and using the electric field in the corotation frame of reference $E' = \Delta u B_J$:

$$K_\perp = \Sigma_{\perp iono} E' \quad \text{or} \quad \Delta u = K_\perp / (\Sigma_{\perp iono} B_J). \tag{8.123}$$

Note that the E-region ionospheric scale height is approximately $H_{iono} \approx 200$ km. Reviewing Section 7.3.8 on ionospheric conductivity we find that the height-integrated conductivity can be approximated as $\Sigma_{\perp iono} \approx H_{iono} \sigma_{\perp iono(maximum)}$. The maximum Pederson conductivity is roughly $\sigma_{\perp iono(maximum)} \approx n_e e / B_J \approx 3 \times 10^{-16} n_e$ in SI units, where n_e is the electron density at the altitude where the ion

gyrofrequency equals the collision frequency ($\nu_i \approx \Omega_i$), which for Jupiter is where the neutral density is about $10^{14}\ cm^{-3}$. This is in the 300–400 km region, which is in the lower ionosphere. The electron density in the Jovian E-region is very uncertain, especially at these altitudes and at high latitudes that are subject to auroral precipitation. We adopt $n_e \approx 10^4\ cm^{-3}$. The major ion species probably is H_3^+ or hydrocarbon ions. A quick estimate gives $\sigma_{\perp iono(maximum)} \approx 3 \times 10^{-6}$ S/m, and using $H_{iono} \approx 200$ km, we find that $\Sigma_{\perp iono} \approx 0.6$ S. The height-integrated current density determined from the total current is $K_\perp \approx I/\pi R_J \approx 0.005$ A/m, where I is the total current found in Example 8.5. Putting this all together, Equation (8.123) predicts that $\Delta u \approx 200$ m/s so that $\Delta u/u = \Delta u/u_n \approx 1\%$. The departure from corotation in the Io plasma torus and in the magnetically connected ionosphere is quite small. Note that this is really a departure from the motion of the neutral gas. If zonal winds exist then this also gives a departure from strict corotation even if $K_\perp = 0$.

8.7.3.2 *Vertical force balance*

Now we consider the component of Equation (8.119) orthogonal to the equatorial plane of the magnetosphere. We assume that the magnetic and rotational equators are identical, which is not quite true since the dipole tilt angle is 9.6°. We need to analyze the force balance along the magnetic field direction, which is *almost* the same as being in the normal/vertical direction. In the direction along the magnetic field $\mathbf{J} \times \mathbf{B} \approx \mathbf{0}$, so that we can write the force balance as

$$\rho \boldsymbol{\Omega} \times (\boldsymbol{\Omega} \times \mathbf{r}) \cdot \hat{\mathbf{b}} \cong -\frac{\partial p}{\partial z}. \tag{8.124}$$

We see from Figure 8.51 that a plasma density gradient exists in the z direction. For an isothermal gas the plasma pressure gradient is also in the z direction. The pressure gradient force is directed *outward* (up and down) from the equatorial plane. This is balanced by the component of the centrifugal force parallel to the magnetic field, which is primarily directed inward toward the equatorial plane.

Equation (8.124) can be used to derive (Bagenal, 1992) an expression for the electron density as a function of height above the equatorial plane (z). We first assume that the plasma pressure (electron plus ion) is given by $p \approx 2 n_e k_B T_i$, where $T_e = T_i$ is assumed. Then, the component of the centrifugal force along the magnetic field direction can be determined by employing expressions for the components of a dipole magnetic field component given in Chapter 3. In Problem 8.27 you will show that near the equatorial plane, $\hat{\mathbf{n}} \cdot \hat{\mathbf{b}} \cong 3z/r$, where the $\hat{\mathbf{n}}$ vector is parallel to the centrifugal force, which is directed outward from the rotation axis. You can also then show that for an isothermal gas (and working with positive z only), Equation (8.124) becomes $n_e m_i \Omega^2 3z = -2k_B T_i (\partial n_e / \partial z)$. Integrating, we find that the electron density as a function of distance z above the plane varies exponentially

with scale height H_z as

$$n_e(z) = n_{e0} \exp(-z^2/H_z^2) \quad \text{with } H_z = \sqrt{\frac{4k_B T_i}{3m_i \Omega^2}}. \tag{8.125}$$

If the electron pressure were omitted in this derivation, then a factor of 2 would appear in the numerator of H_z in Equation (8.125) rather than the factor of 4 that appears there now.

The value of H_z depends on temperature and is obviously greater in the outer plasma torus than it is in the inner torus because T_i is higher in the former than in the latter. Equation (8.125) predicts that $H_z \approx 1\ R_J$ in the outer torus and that H_z is only about 0.1 R_J in the cold inner torus. These scale height values basically agree with the electron density data displayed in Figure 8.51.

8.7.3.3 Radial momentum balance

Now let us consider the radial component of the momentum Equation (8.119): $[\mathbf{J} \times \mathbf{B}]_r = \partial p/\partial r + [\rho\boldsymbol{\Omega} \times (\boldsymbol{\Omega} \times \mathbf{r})]_r$. We restrict ourselves to the equatorial plane of the magnetosphere for simplicity. The mass-loading term is assumed to be zero because we made the assumption that the plasma flow is entirely azimuthal. The relevant component of $\mathbf{J}$ is the azimuthal component J_ϕ. In terms of J_ϕ the momentum equation can now be written as

$$J_\phi = \frac{1}{B}\left[-\frac{\partial p}{\partial r} + \rho\Omega^2 r\right], \tag{8.126}$$

where we can also write $\partial p/\partial r = (1/R_J)\,\partial p/\partial L$.

The force balance represented by Equation (8.126) basically states that an outward pressure gradient force (assuming that p decreases with increasing radial distance) plus an outward centrifugal force on the plasma are countered by an inward $\mathbf{J} \times \mathbf{B}$ force associated with an azimuthal electrical current. This current is a *ring current*, in that it encircles Jupiter in the plasmasheet. Figure 8.53 illustrates this force balance schematically.

We now consider Equation (8.126) in more detail. In Example 8.7 we consider the Io plasma torus region ($L \approx 6$–8) and use the data shown in Figure 8.51 (assuming $T_e = T_i$) to find the pressure p of the thermal population and the density ρ. We find that the total "ring" current in the Io plasma torus is roughly 20 MA.

Example 8.7 (Azimuthal electrical current estimate at $L \approx 7$ in the Io plasma torus) Equation (8.126) and the data from Figure 8.51 can be used to estimate a typical current density in the Io plasma torus and the total azimuthal current I_ϕ between about $L = 6$ and $L = 8$.

The pressure in the L = 6–8 region is roughly 5×10^{-8} N/m^2 taking into account both T_e and T_i, and the radial pressure gradient is roughly $(1/R_J)\partial p/\partial L \approx \Delta p/(\Delta L R_J) \approx (5 \times 10^{-8}\ \text{N/m}^2)/(2 \times 7 \times 10^7\text{m}) \approx 4 \times 10^{-16}$ N/m^3. The mass density near $L = 7$ is roughly $\rho = m_i n_e \approx 25\,\text{amu} \times 1.66 \times 10^{-27}\,\text{kg/amu} \times 10^3\,\text{cm}^{-3} \times 10^6\,\text{cm}^3\text{m}^{-3} \approx 4 \times 10^{-17}$ kg/m^3, and the centrifugal force per unit volume can be estimated as $\rho\Omega^2 r \approx \rho(1.77 \times 10^{-4}\,\text{s}^{-1})^2\,7R_J \approx 6 \times 10^{-16}$ N/m^3. Our average mass ($\langle m_i \rangle \approx 25$ amu) assumed roughly comparable abundances of S and O ions. The centrifugal force term is comparable to the pressure gradient term, although the contribution of energetic particles to the pressure has *not* been taken into account. Equation (8.126) can now be used to estimate J_ϕ in the Io plasma torus: $J_\phi = [4 \times 10^{-16}\ \text{N/m}^3 + 6 \times 10^{-16}\ \text{N/m}^3]/B = 10^{-15} \times L^3/B_J \approx (3.5 \times 10^{-13}\ \text{N/m}^3)/(4 \times 10^{-4}\,\text{T}) \approx 10^{-9}\text{Am}^{-2}$. The cross-sectional area of the Io torus for $L = 6$–8 is *area* $\approx \Delta z \Delta L R_J \approx 4R_J^2 \approx 2 \times 10^{16}$ m^2. The total "ring" current for this region is then

$$I_\phi \approx \textit{area} \times J_\phi \approx 20\,\text{MA}. \tag{8.127}$$

This Jovian ring current encircles Jupiter just as the terrestrial ring current encircles the Earth, but in the opposite direction, although the dynamical "drivers" are different for these currents.

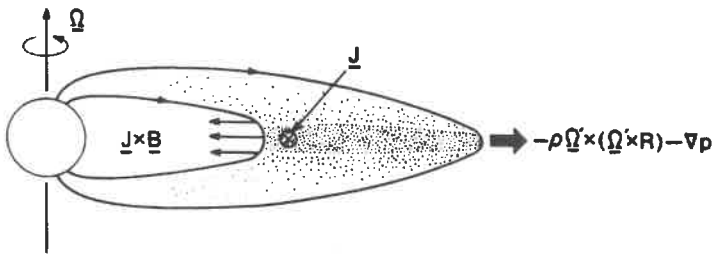

Figure 8.53. Schematic showing radial force balance in the Jovian plasmasheet. An inward $\mathbf{J} \times \mathbf{B}$ force balances an outward pressure gradient force plus an outward centrifugal force on the corotating plasma. (From McNutt, 1983.) Reprinted from *Advances in Space Research*, vol. 3, R. L. McNutt, p. 55, copyright 1983, with kind permission from Elsevier Science Ltd., The Boulevard, Langford Lane, Kidlington OX5 1GB, UK.

Energetic ion populations are present in the Jovian magnetosphere as well as the relatively cold but dense thermal ion population, especially beyond $L = 10$, and we know that for the terrestrial ring current the energetic ion population makes the dominant contribution to the pressure and to the electrical current. Information on the Jovian energetic ion population is minimal, which makes it difficult to determine the associated electrical current accurately. But as discussed by Vasyliunas (1983), instead of using Equation (8.126), the procedure can be reversed and Equation (8.126) can be used to estimate the pressure if the current density can be estimated independently. Comparison of magnetic field vectors measured along

the *Pioneer* and *Voyager* spacecraft trajectories with the magnetic field expected for a simple tilted dipole provides an empirical determination of the current density **J**, from which the variation of the pressure can be estimated. This method was used by several researchers to estimate the pressure in the plasmasheet (and current sheet), as discussed in the book *Physics of the Jovian Magnetosphere* (Dessler, 1983). For the range $L \approx 8$–80 this empirical pressure variation can crudely be represented by the following function of L-shell:

$$p \approx 150\,\text{keV/cm}^3 \quad [10/L]^4. \tag{8.128}$$

The actual deduced pressure variation (e.g., Vasyliunas, 1983) depends on the empirical magnetic field model that is used and has a somewhat more complex variation than is exhibited by Equation (8.128). In SI units, Equation (8.128) is $p = 2.5 \times 10^{-8}\,[10/L]^4\ \text{N/m}^2$.

At $L \approx 7$ the simple formula (8.128) predicts that $p \approx 10^{-7}\ \text{N/m}^2$, which is about a factor of two greater than the value we estimated from the measured thermal plasma parameters in this region; however, the more energetic plasma also makes some contribution to the pressure, even at $L \approx 7$. The energetic plasma becomes especially important for L values greater than about 10. Equation (8.128) includes pressure contributions from *all* particle populations. The pressure contribution from ions (e.g., H^+ and O^+) in the 28 keV to 4 MeV energy range has been evaluated for the nightside portion of the Jovian plasmasheet using ion fluxes measured by instruments on board *Voyagers 1* and *2* (see Paranicas et al., 1991). This pressure roughly agrees with Equation (8.128), confirming the importance of the contribution of the more energetic ions.

Equation (8.128) can be used to estimate the plasma beta as a function of L with the assumption of a dipole magnetic field:

$$\beta = p/(B^2/2\mu_0) \approx 2 \times 10^{-3} L^2. \tag{8.129}$$

At $L \approx 7$, Equation (8.129) predicts that $\beta \approx 0.1$. Equation (8.129) indicates that β exceeds unity only for $L > 22$. Hence, beyond about $L \approx 20$ the magnetic field is strongly affected by the electrical current flowing in the plasmasheet, and the dipole field formula used to derive Equation (8.129) is no longer valid. Nonetheless, if we use it anyway to estimate β near the magnetopause ($L \approx 60$), we find that $\beta \approx 6$, which is roughly correct. This is also the value of β we used in Chapter 7 to estimate the magnetopause location for Jupiter.

The simple pressure formula (8.128) can also be used together with Equation (8.126) to estimate the azimuthal electrical current in the plasmasheet of the "middle magnetosphere" ($L \approx$ 10–20). This is an oversimplification, which we will overlook for now. To use Equation (8.128) we need to know how the density ρ varies with L in order to evaluate the centrifugal force contribution to the current.

Using *Voyager* data as reviewed by Bagenal (1985), the following formula can be devised and provides a crude estimate of the L-shell variation of the electron density in the plasmasheet for $L \approx$ 10–20:

$$n_e \approx 50\,\text{cm}^{-3}\,[10/L]^3. \tag{8.130}$$

This formula underestimates the electron density for $L < 10$ (by about a factor of four at $L = 7$). Using this equation plus the pressure formula, as well as adopting a dipole magnetic field, we can derive an approximation for the current density of

$$J_\phi \approx 3 \times 10^{-8} L^{-2} + 10^{-11} L \quad [\text{Am}^{-2}], \tag{8.131}$$

where the first term is from the pressure gradient force and the second term is from the centrifugal force. At $L \approx 10$ we find that $J_\phi \approx 4 \times 10^{-10}\ \text{A/m}^2$ with the pressure term being a factor of three greater than the centrifugal term. By $L \approx 20$, Equation (8.131) indicates that $J_\phi \approx 3 \times 10^{-10}\ \text{A/m}^2$ with the centrifugal term being three times greater than the pressure term. The two terms cross over in importance at about $L \approx 15$.

The total ring current carried in the region between $L = 10$ and 20 can be found by integrating Equation (8.131) from $L = 10$ to 20 over a suitable cross-sectional area (e.g., 2 R_J). This procedure gives a total current of about 30 MA.

The above picture is oversimplified. For example, the magnetic field is not really dipolelike due to the large electrical currents flowing in the plasmasheet, and the pressure is not really isotropic. And there is evidence that, at least on the nightside, the relative importance of the centrifugal force term is less than is indicated by Equation (8.131) (Paranicas et al., 1991; McNutt, 1983). The momentum equations (2.59) and (2.61) contain the divergence of a *pressure tensor* for species s, $\nabla \cdot \tilde{\mathbf{P}}_s$, but with one exception (Section 3.10.3) we have adopted isotropic pressure ($p_\parallel = p_\perp$) throughout this book. Recall that $p_\parallel$ and $p_\perp$ are the parallel and perpendicular pressures, respectively. Paranicas et al. (1991) demonstrated that the radial component of the pressure force $-\nabla \cdot \tilde{\mathbf{P}}_s$ can be expressed as

$$F_r = -\frac{\partial p_\perp}{\partial r} + \frac{p_\perp}{R_c}\left(\frac{p_\parallel}{p_\perp} - 1\right), \tag{8.132}$$

where R_c is the radius of curvature of the magnetic field lines (also see Equation (3.42)). The first term of Equation (8.132) was already included in Equation (8.126) but the second term is new, and according to Paranicas et al. (1991), it is several times more important than the first term for the nightside Jovian neutral sheet. These authors estimate that $p_\parallel/p_\perp \approx 1.2$ and that $R_c \approx 0.5\ R_J$ near $L \approx 20$. Hence the second term in Equation (8.132) is $\approx 0.4(p_\perp/R_J)$, whereas the first term is $\approx 4p_\perp/(LR_J) \approx 0.2(p_\perp/R_J)$.

8.7.4 Radial plasma transport in the Jovian magnetosphere

In considering the momentum balance in the way we did, the plasma was assumed to be purely corotating, in which case the plasma density is solely determined by local production and loss processes. Local production and loss processes are indeed very important in the Io plasma torus, but radial plasma transport is also important (cf. Bagenal, 1992). However, radial transport is thought to take place primarily as a diffusion process rather than as "organized convection." An important exception to this is thought to exist in the tail for $L > 50$, where the centrifugal force overwhelms the capacity of the inward $\mathbf{J} \times \mathbf{B}$ force to counteract it such that bulk plasma transport down the Jovian magnetotail takes place.

The radial transport Equation (3.105) for cross-L-shell diffusion is applicable to the Jovian magnetospheric plasma, although source and sink terms must be added. A steady-state version of Equation (3.105) can be written for the pitch-angle-averaged distribution function in the equatorial plane:

$$L^2 \frac{\partial}{\partial L}\left(\frac{D_{LL}}{L^2}\frac{\partial f}{\partial L}\right) - \frac{f}{\tau_{net}} = 0, \tag{8.133}$$

where D_{LL} is the cross-L-shell diffusion coefficient. The distribution function, $f(E, L)$, for any given particle species (mainly S or O ions in this case) can be expressed as a function of particle energy and L-shell. At lower energies, the distribution function is that of the thermal plasma, but at higher energies, in the "tail" of the distribution, the ring current and radiation belt populations are being represented.

The "net" local production time constant, or lifetime, τ_{net}, takes into account all local production and loss processes as a function of particle energy. For the thermal particles, collisional production and loss are the most important processes, and these are mainly associated with the Io plasma torus. However, for the energetic particles, the loss mechanisms include encounters with the satellites of Jupiter and losses due to pitch-angle scattering into the loss cone. The latter process results in the precipitation of energetic particles into the upper atmosphere of Jupiter. In fact, auroral emissions from the polar regions of Jupiter have been observed by the ultraviolet spectrometers on the *Voyager 1* and 2 spacecraft as well as by the Earth-orbiting *International Ultraviolet Explorer (IUE)* satellite and the *Hubble Space Telescope* (c.f. Nagy et al., 1995). The total power of the Jovian aurora estimated from these observations is about 10^{13}–10^{14} W, which is a factor of 10 to 100 greater than the total power of the terrestrial aurora. Radio emissions in several frequency bands have also been observed from the Jovian magnetosphere, and some of these emissions are associated with the Io torus and with the aurora (cf. Bagenal, 1992).

It is not known how the energetic particles in the Jovian magnetosphere, some of which are responsible for the aurora, are accelerated, although several different theories have been put forth. Particles can be accelerated in a variety of ways. In particular, two processes can alter the energy of a charged particle undergoing radial transport:

(1) *Betatron acceleration* can occur – a particle transported to a lower L-shell has its perpendicular kinetic energy increased as the magnetic field strength increases if the first adiabatic invariant ($\mu_m = \frac{1}{2}mv_\perp^2/B$) is conserved during the transport process. If wave–particle scattering makes the distribution function isotropic so that parallel and perpendicular energy are equipartitioned, then the adiabatic relation (Example 8.4) applies and predicts plasma energization.

(2) The *corotation electric field* can also energize plasma. We saw that ions born in the Io plasma torus gain a few hundred eV from the corotating Jovian magnetic field and the associated corotation electric field. The corotation energy, $E_{corot} = 1/2m\Omega^2r^2$, increases as r^2 (or L^2). Outward diffusion should lead to energy gain from this process. Of course in a corotating reference frame this is *not* an energy gain. Furthermore, adiabatic cooling from process (1) can counteract this energy gain.

Radial diffusion transport times estimated for the Jovian magnetosphere are in the range of about 10–100 days for the thermal part of the plasma for $L > 5.7$ and are a few years for $L < 5.7$. The cross-L diffusion coefficients used by researchers have been mainly determined empirically, but speculation concerning the responsible physical processes has centered on the *magnetic flux tube interchange instability*, which is a macroscopic MHD instability that can be driven by the outwardly directed centrifugal force. This topic will not be considered here, but given a diffusion coefficient you recall that the transport time can be estimated as $\tau_{trans} \approx \Delta L^2/D_{LL}$, where ΔL is the interval over which the diffusive transport takes place. An average radial speed for the plasma can be estimated as $\langle u_r \rangle \approx R_J \Delta L/\tau_{trans}$. Using reasonable values of $\tau_{trans} = 30$ days and $\Delta L \approx 5$, we find that $\langle u_r \rangle \approx 0.1$ km/s. Our earlier assumption that the corotational motion is dominant is indeed valid given that $\langle u_r \rangle / u_{corot} = \langle u_r \rangle / (\Omega R_J L) \approx 10^{-3}$ near the Io plasma torus. Nonetheless, although $\langle u_r \rangle \ll u_{corot}$, the radial motion plays an important role in determining the particle distribution function in the Jovian magnetosphere.

The processes operating in the Saturnian magnetosphere are very similar to what has just been discussed for Jupiter, except that instead of an Io plasma source Saturn has plasma sources associated with its rings and with Titan. NASA's *Galileo* spacecraft went into orbit around Jupiter in December 1995 and is now making measurements of the particles and fields in the Jovian magnetosphere. And it is expected that the *Cassini* spacecraft will go into orbit around Saturn in the year 2004. Our knowledge of the magnetospheres of Jupiter and Saturn will certainly greatly increase because of the data returned by these two missions.

Problems

8.1 Derive Equation (8.5) for $d\rho/\rho$ from information found in Section 6.2.1. For strongly subsonic flow ($M^2 \ll 1$), show that this is equivalent to $dM/M = -dA/A$.

8.2 Show that in steady state and for cylindrical geometry, $\nabla \cdot (B\mathbf{u}) = 0$, for infinite electrical conductivity. The magnetic field is assumed to be aligned

with the axis of the cylinder. For incompressible flow, demonstrate that this implies that $B \approx$ *constant*.

8.3 **Determination of Alfvénic Mach number for the plasma flow into the reconnection region** Combine Equations (8.14) and (8.17) to obtain an algebraic equation for $M_{A0\,max}$:

$$M_{A0\,max} = \frac{\pi}{8} \frac{1}{\ln\left(\frac{r_{mp}}{r_L}\right) - \ln(M_{A0\,max})}.$$

Solve this equation iteratively and show that $M_{A0\,max} \approx 0.04$ for the values of the parameters discussed in the text. What happens to $M_{A0\,max}$ if larger values of either r_{mp} or the width of the diffusion region a are employed instead of the values tried in the text?

8.4 Estimate values for the parameters b, d, and L that appear in Figure 8.7.

8.5 Demonstrate that the *Poynting vector* (see the appendix for a review of electromagnetic theory) can be used to derive Equation (8.22). Also derive Equation (8.25).

8.6 Review Chapter 3 and demonstrate that the total amount of energy in the ring current is about 10^{15} J for moderately active conditions.

8.7 Use the reconnection formalism (e.g., u_0, etc.) to demonstrate that the power conversion of magnetic to kinetic energy at the dayside magnetopause via reconnection is, indeed, for southward IMF, about equal to $P_{sw-m} \approx 10^{11}$ W.

8.8 **Derivation of the electron inertial length** Derive Equation (8.27) for a sharp interface between a magnetized region that is a vacuum and an unmagnetized plasma region. Assume equal electron and ion temperatures. Consider what electric potential is needed to repulse the incident protons and use a simple generalized Ohm's law, $\mathbf{E} = -\mathbf{u}_e \times \mathbf{B}$, where $\mathbf{u}_e$ is the bulk flow velocity of the electrons. Sketch the current layer showing $\mathbf{E}$, $\mathbf{u}_e$, and the current density $\mathbf{J}$.

8.9 Demonstrate that for an ionosphere with uniform electrical conductivity the Hall current makes a negligible contribution to the field-aligned current into (or out of) the top of the ionosphere.

8.10 Repeat the analysis of Section 8.3 for a scenario in which the top plasma slab has a thickness of $3H$ rather than H. Assume that all other parameters remain the same. Assume that for the top slab $\partial u_0/\partial t = 0$ but $\partial p/\partial y \neq 0$. Determine both u_0 and u_1 (i.e., the flow speeds in the top and bottom slabs, respectively) as well as the electric field strength and the current densities.

8.11 Derive an ordinary differential equation for the velocity function $u_0(t)$ in Section 8.3.3 and show that Equation (8.50) is the solution. Also derive Equation (8.66).

8.12 (a) Demonstrate that Equations (8.69)–(8.71) are consistent with Equation (8.60).
(b) Derive Equations (8.73) and (8.74) given the simplifying assumptions made in Section 8.4.

8.13 Derive Equations (8.86) and (8.88). Then find the plasmapause L-shell, L_{pp}, for *all* local times rather than just 18:00 LT as was done in the text.

8.14 **Plasmaspheric refilling times** The ionospheric source (i.e., upward flux) of H^+ ions produced by the reaction of O^+ ions with neutral atomic hydrogen can be found by integrating over altitude the production rate, $P = k[O^+][H]$, where the reaction rate coefficient $k = 6 \times 10^{-10}$ cm^{3}s^{-1}, where the hydrogen density is approximately [H] $\approx 10^5$ cm^{-3} (almost constant in F-region altitude range), and where the peak O^+ density is [O^+] $\approx 10^6$ cm^{-3}. Show that the H^+ flux upward into the plasmasphere is approximately given by: *flux* $\approx P H_p \approx 10^9$ cm^{-2} s^{-1}. Estimate plasmaspheric refilling times for $L = 2, 3, 4$, and 5.

8.15 Estimate the trajectories of H^+, He^+, and O^+ ions that start out in the polar ionosphere with an average energy (i.e., temperature) of 30 eV and then move out into the magnetosphere. Sketch the trajectories (in the noon–midnight plane) you have found. Assume a cross-tail magnetospheric potential of 100 kV and use dipole magnetic field lines.

8.16 Derive the electromagnetic energy conservation equation (A.45) from Maxwell's equations.

8.17 Show that the dynamical pressure term, the frictional force term, and the gravitational term can be neglected in the momentum balance for the terrestrial plasmasheet at a radial distance of about 20 R_E. Take information as needed from the tables and figures of Chapter 8. Assume a neutral hydrogen density of about 1 cm^{-3} at this location.

8.18 Estimate the gyroradius of a typical plasmasheet proton near the neutral sheet (a) for a constant field $|B_z| = 3$ nT and (b) as a function of L from $L = 6$ to $L = 20$ for a dipole field. Show that the adiabatic invariants (Chapter 3) might not be conserved right in the neutral sheet where the length scale for significant field changes is roughly 1 R_E. The resulting proton trajectories are "chaotic" and could play an important role in the plasmasheet dynamics during magnetic substorms when the plasmasheet is especially thin.

8.19 Estimate the height-integrated Hall current density in the auroral oval, K_H, and also the total Hall current near the auroral oval. Assume a magnetospheric potential of $\Psi_m = 100$ kV and a width of the oval of about 5° latitude. Making the approximation that all this current runs in a thin filament (like a wire) along the auroral oval at an altitude of 100 km, estimate the magnetic perturbation at the ground due to this *auroral electrojet* current. Demonstrate that the Hall currents flow along equipotential lines in a direction opposite to the polar cap plasma convection.

8.20 Apply Equation (8.111) to the plasmasheet electron and proton populations and find the maximum current density that can be carried by these particle populations (e.g., for electrons from Table 8.1, $n_e \approx 1\,\mathrm{cm}^{-3}$ and $T_e \approx 1\,\mathrm{keV}$). Also apply this equation to upward flowing ionospheric O^+ ions originating in the topside ionosphere and show that $J_{max} \approx 0.5\,\mu\mathrm{A/m}^2$.

8.21 Review the treatment of kinetic theory in Chapter 2 and then demonstrate that charged particles accelerated by a one-dimensional electrostatic field (either $B = 0$ or only motion parallel to B is considered) conserve their flux in the direction of this field. That is, the flux of particles of species s is given by $n_s u_{sx} = constant$ (in the x direction) if the electrostatic field is in the x direction.

8.22 Consider two locations on a magnetic field line with radial distances $r_2 > r_1$. The magnetic field strength at r_2 is only 20% of the field strength at r_1; that is, $B(r_2) = 0.2B(r_1)$. Suppose we start with an isotropic flux of monoenergetic 1 keV electrons at r_2. The electron density at r_2 is $1\,\mathrm{cm}^{-3}$. Calculate the loss cone angle for the distribution at r_2 assuming that all electrons are somehow physically absorbed at r_1. Also calculate the electron flux parallel to the field at both r_1 and r_2. Now assume that the electrons are accelerated by an electrostatic field in the direction parallel to the magnetic field. Assume that the field-aligned potential drop occurs in a narrow region ($\Delta r \ll r_2$) located just below r_2. Estimate the electron flux parallel to the magnetic field both at r_1 and r_2.

8.23 Estimate the energy flux into the atmosphere associated with the differential electron flux shown in Figure 8.48. Near what altitude is most of the energy deposited? Use Equation (8.103) to estimate the electrical conductivity of the auroral ionosphere associated with this particular auroral precipitation event. About how many ion pairs are produced in a vertical column with cross-sectional area $1\,\mathrm{cm}^2$? Dividing this column ion production rate by a typical scale height in the lower thermosphere (15 km), you can also get a crude estimate of the total ion production rate, and then by assuming that dissociative recombination ultimately removes ionospheric plasma in the E-region you can also photochemically estimate the peak ionospheric electron density. How does this compare with nonauroral E-region electron densities?

8.24 Derive for planet "x" the following formula for the critical speed at which the corotation speed at an L-shell matches the magnetic curvature and gradient drift speed v_B:

$$v_{crit}^2 \approx \Omega_{gyro}\Omega_{rotation}R_x^2L^2,$$

where R_x is the radius of the planet, $\Omega_{rotation}$ is the rotational frequency, and Ω_{gyro} is the gyrofrequency at that L value. Evaluate the critical energy ($(1/2)mv_{crit}^2$) for protons at $L = 6$ in the terrestrial plasmasphere and for oxygen ions at $L = 10$ in the Jovian magnetosphere.

8.25 Determine the surface magnetic field strength at the magnetic equators of all the outer planets given the data in Table 7.1 and assuming that the field is given by a simple magnetic dipole.

8.26 Calculate the gyroperiod, bounce period, and drift period of 50 MeV protons at $L = 10$ in the Jovian radiation belts. Assume a pitch angle of 45°. Compare your results with the terrestrial values in Table 3.1.

8.27 Show that $\hat{\mathbf{n}} \cdot \hat{\mathbf{b}} \cong 3z/r$ near the equatorial plane of a magnetosphere of a planet with a dipole magnetic field, where the $\hat{\mathbf{n}}$ vector is parallel to the centrifugal force, which is directed outward from the rotation axis, r is the radial distance, and z is the height above the rotational (and magnetic) equatorial plane.

8.28 Derive Equation (8.131) and then use Equation (8.132) to find a new version of Equation (8.131). Estimate and then plot the current density versus L value for the Jovian magnetosphere.

8.29 Calculate the corotation speed (and energy) for Jovian oxygen ions and Saturnian nitrogen ions and plot these speeds versus L value. Do this for $L = 1$ to 60 for Jupiter and $L = 1$ to 25 for Saturn.

8.30 Consider a hypothetical Saturn whose rotational frequency is only 0.1% that of the real Saturn; all other parameters are the same. Estimate the distance to the plasmapause (L_{pp}) for this planet. Estimate the magnetospheric electric field due to the solar wind assuming an open magnetosphere model and a reasonable dayside magnetopause magnetic reconnection efficiency. What is the direction of this electric field? What is the cross-tail magnetospheric potential? Sketch the magnetospheric plasma convection pattern in the equatorial plane.

8.31 Let us suppose that Titan supplies 10^{25} N atoms per second to a torus centered R_S at the orbital distance of Titan (20.3 R_S) and with an extent (or minor radius) of ± 1 R_S. These ions are all eventually ionized and thus contribute to the mass-loading of the magnetosphere near $L \approx 20$. Estimate the total electrical current associated with this mass-loading. Assume that Saturn's ionospheric properties are the same as was assumed for Jupiter in the text.

Bibliography

Arnoldy, R. L., P. B. Lewis, and P. O. Isaacson, Field-aligned auroral electron fluxes, *J. Geophys. Res.*, **79**, 4208, 1974.

Axford, W. I. and C. O. Hines, A unifying theory of high-latitude geophysical phenomena and geomagnetic storms, *Can. J. Phys.*, **39**, 1433, 1961.

Bagenal, F., Planetary magnetospheres, p. 224 in *Solar System Magnetic Fields*, ed. E. R. Priest, D. Reidel Publ. Co., Dordrecht, The Netherlands, 1985.

Bagenal, F., Giant planet magnetospheres, *Annu. Rev. Earth Planet. Sci.*, **20**, 289, 1992.

Baumjohann, W., Ionospheric and field-aligned current systems in the auroral zone: A concise review, *Adv. Space Res.*, Vol. 2, No. 10, 55, 1982.